

## Electronic Supplementary Information

# 1,1,1,3,3,3-Hexafluoro-2-propanol (HFIP) as a novel and effective solvent to facilely prepare cyclodextrin-assembled materials

*Toshiyuki Kida, Shin-ichiro Sato, Hiroaki Yoshida, Ayumi Teragaki and Mitsuru Akashi\**

*Department of Applied Chemistry, Graduate School of Engineering, Osaka University, 2-1 Yamada-oka,  
Suita 565-0871, Japan*

### Contents

1. Materials and methods	S2
2. <sup>1</sup> H NMR spectra of CDs regenerated from the CD/HFIP solutions	S3
3. <sup>1</sup> H-NMR spectral changes observed for CDs in D <sub>2</sub> O upon addition of HFIP	S3-4
4. <sup>1</sup> H-NMR titration curve for complex formation between β-CD and HFIP in D <sub>2</sub> O	S5
5. Job plot for a complex between β-CD and HFIP in D <sub>2</sub> O	S5
6. Photographs of CD/HFIP solutions and CD crystalline solids obtained from the HFIP solutions	S6
7. XRD patterns of CD solids obtained by the freeze-drying of CD/HPIC solutions	S7
8. XRD patterns of the micrometer-sized CD beads formed by electrospinning of HFIP solutions	S7
9. SEM image of β-CD structures formed by electrospinning of a 10 wt% β-CD/HFIP solution	S8

## 1. Materials and methods

$\alpha$ -,  $\beta$ - and  $\gamma$ -CD were purchased from Wako Pure Chemical Industries Ltd. (Japan) and dried overnight at 80 °C under a reduced pressure before use. 1,1,1,3,3,3-hexafluoro-2-propanol (HFIP), 1,1,1,3,3,3-hexafluoro-2-methyl-2-propanol (HFMP) and 2,2,2-trifluoroethanol (TFE) were purchased from Wako Pure Chemical Industries Ltd. (Japan).

The solubilities of CDs in fluorinated alcohols were determined by visually estimating the saturation concentration through the addition of a prescribed amount of CD into a fluorinated alcohol (2 mL) and subsequent stirring for 1 h.

The  $^1\text{H-NMR}$  titrations were performed at 25 °C in  $\text{D}_2\text{O}$ . A solution of the CD molecule (0.6 mL, 1.0 mM) was titrated in a NMR tube with increasing amounts of HFIP stock solution (0.5 mL, 150 mM) as follows (in  $\mu\text{L}$ ): 0, 2.0, 4.0, 8.0, 40, 60, 80. The titration curve (changes in the chemical shift of the  $\beta$ -CD proton ( $\Delta\delta$ ) against the HFIP/ $\beta$ -CD concentration ratio) was analyzed by a non-linear least-squares curve fitting method to generate an association constant of the  $\beta$ -CD-HFIP complex. A Job plot was carried out by monitoring the changes in the chemical shift of the  $\beta$ -CD proton ( $\Delta\delta$ ) in a series of solutions with varying  $\beta$ -CD/HFIP ratios but the total concentration of  $\beta$ -CD and HFIP being kept constant (2.0 mM). The relative concentration of the  $\beta$ -CD-HFIP complex estimated from the  $\Delta\delta \cdot [\beta\text{-CD}]$  value was plotted against  $([\beta\text{-CD}]/\{[\beta\text{-CD}] + [\text{HFIP}]\})$ .

Electrospinning was performed with a Nanofiber Electrospinning Unit (Kato Tech Co., Ltd., Japan). The solution was pumped through a single-use blunt-end 18-gauge cannula at a flow rate of 0.16 mL/min, and the collection distance between the cannula and the rotating drum target (diameter: 10 cm, width: 33 cm) was 10 cm. The drum substrate was covered with aluminum foil and rotated at a rate of 2.0 m/min during the electrospinning of the solutions. A voltage of 25 kV was applied between the cannula and the substrate. The viscosities of the CD/HFIP solutions at different CD concentrations were measured by a viscometer, TOKIMEC TV-20 (Toki Sangyo, Japan).

The morphologies and X-ray diffraction (XRD) patterns of the CD structures obtained via electrospinning were measured by a scanning electron microscope (SEM) (JSF-6701F, JEOL Ltd., Japan) and a Rigaku X-ray diffractometer (Rigaku, Japan), respectively.

## 2. $^1\text{H}$ NMR spectra of CDs regenerated from the CD/HFIP solutions

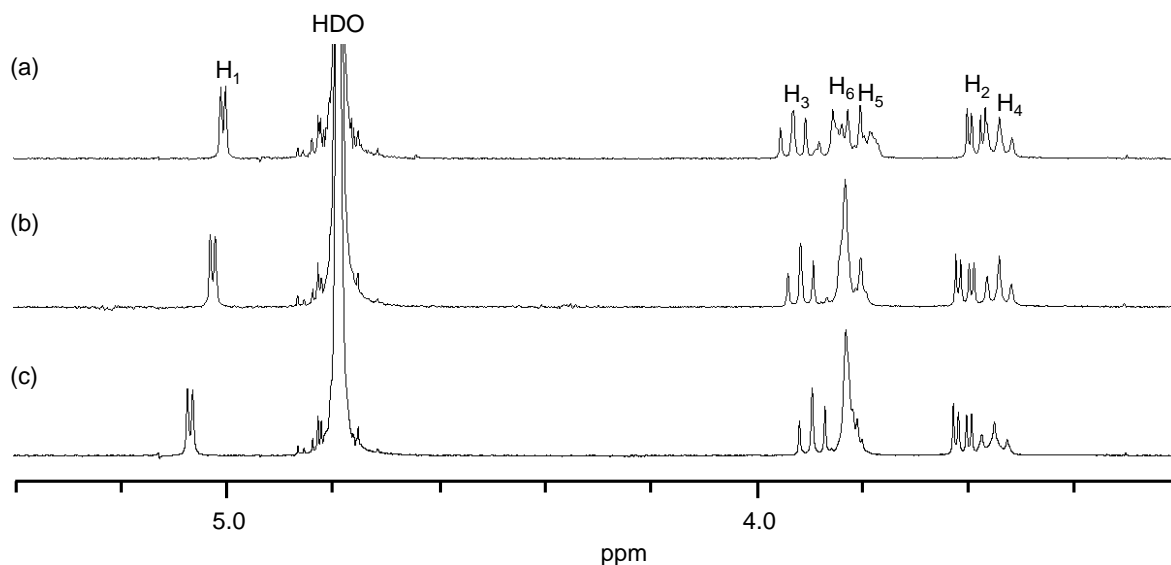


**Fig. S1**  $^1\text{H}$  NMR spectra of (a)  $\alpha$ -, (b)  $\beta$ - and (c)  $\gamma$ -CD regenerated by evaporating HFIP from the corresponding HFIP solutions (solvent:  $\text{D}_2\text{O}$ , CD concentration:  $1.0 \times 10^{-3}$  mol/L).

## 3. $^1\text{H}$ -NMR spectral changes observed for CDs upon addition of HFIP

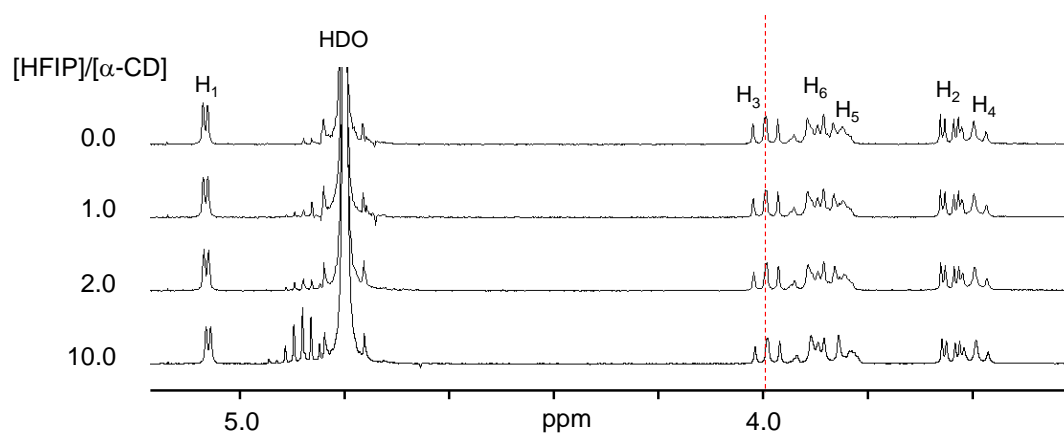


**Fig. S2**  $^1\text{H}$ -NMR spectral changes observed for  $\alpha$ -CD ( $1.0 \times 10^{-3}$  mol/L) upon addition of HFIP in  $\text{D}_2\text{O}$  at  $25^\circ\text{C}$ .

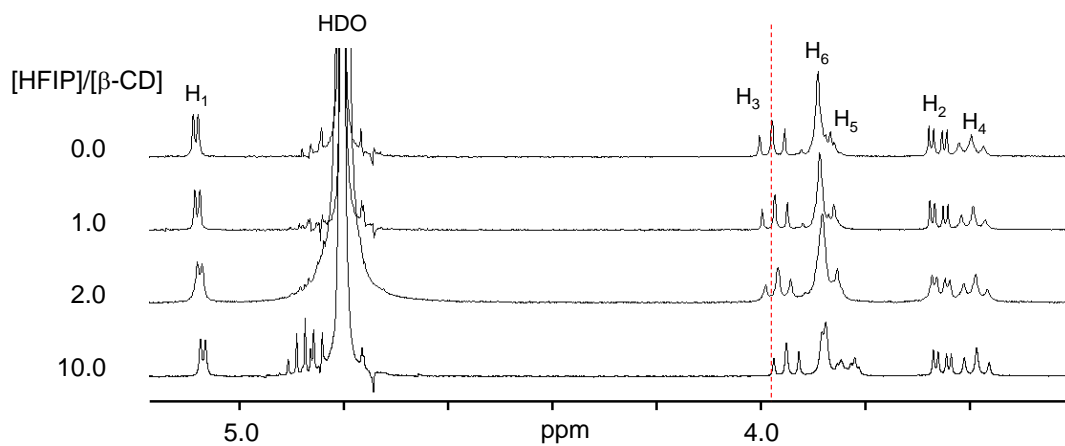


**Fig. S3** <sup>1</sup>H-NMR spectral changes observed for β-CD (1.0 × 10<sup>-3</sup> mol/L) upon addition of HFIP in D<sub>2</sub>O at 25 °C.

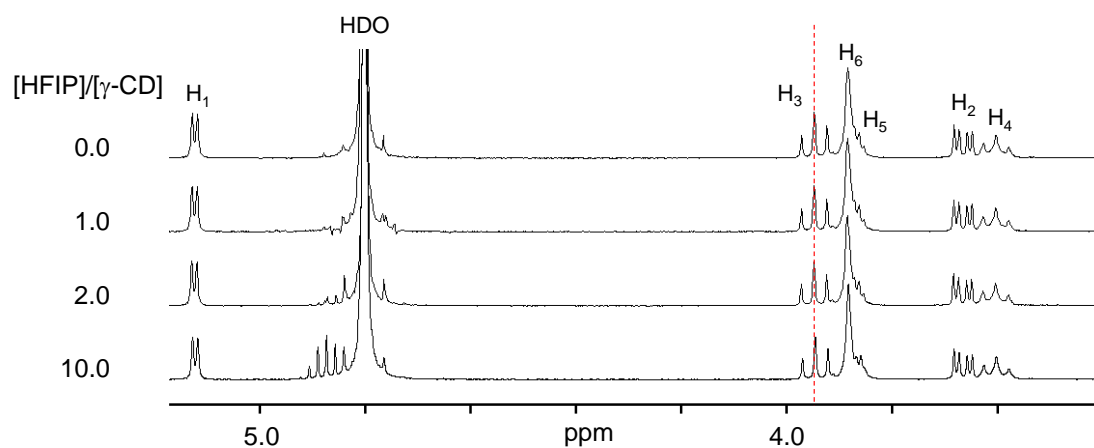


**Fig. S4** <sup>1</sup>H-NMR spectral changes observed for γ-CD (1.0 × 10<sup>-3</sup> mol/L) upon addition of HFIP in D<sub>2</sub>O at 25 °C.

#### 4. $^1\text{H}$ -NMR titration curve for complex formation between $\beta$ -CD and HFIP in $\text{D}_2\text{O}$

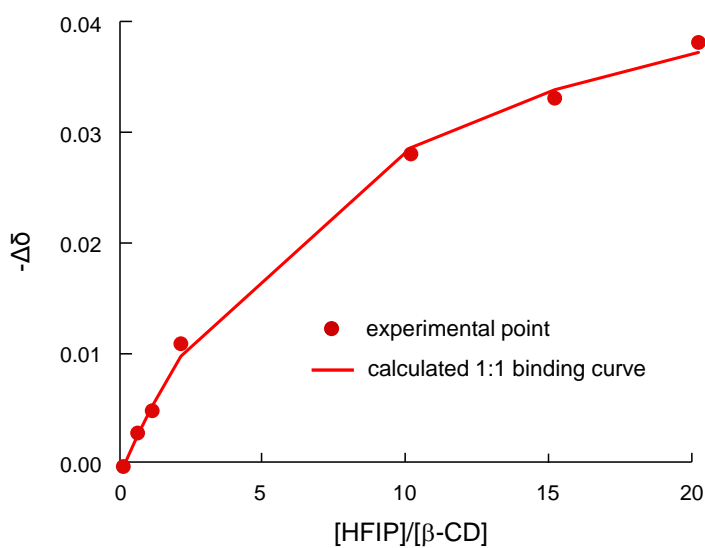


**Fig. S5**  $^1\text{H}$ -NMR titration curve for complex formation between  $\beta$ -CD and HFIP in  $\text{D}_2\text{O}$ . [ $\beta$ -CD] =  $1.0 \times 10^{-3}$  mol/L. At 25  $^\circ\text{C}$ . The  $\text{H}_3$  proton signal of  $\beta$ -CD at 3.98 ppm was used for the titration.

#### 5. Job plot for a complex between $\beta$ -CD and HFIP in $\text{D}_2\text{O}$

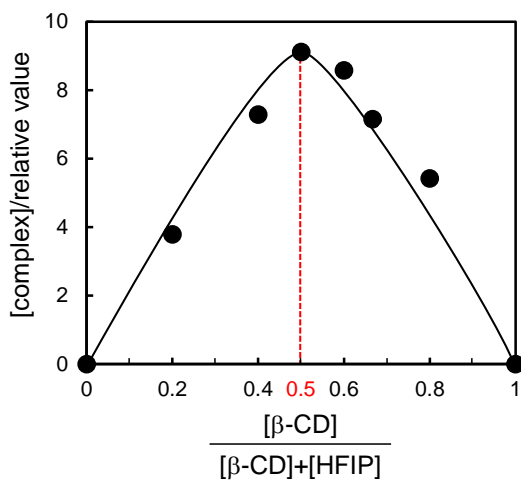


**Fig. S6** Job plot for a complex between  $\beta$ -CD and HFIP in  $\text{D}_2\text{O}$  at 25  $^\circ\text{C}$ .

**6. Photographs of CD/HFIP solutions and CD crystalline solids obtained from the HFIP solutions**

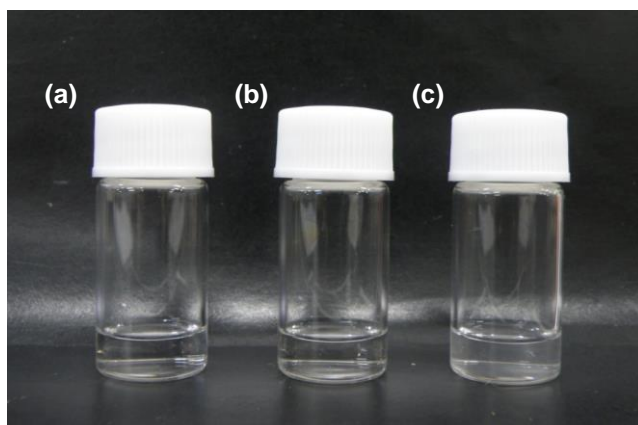


**Fig. S7** Photographs of HFIP solutions of (a)  $\alpha$ -, (b)  $\beta$ - and (c)  $\gamma$ -CD (0.1 mol/L).

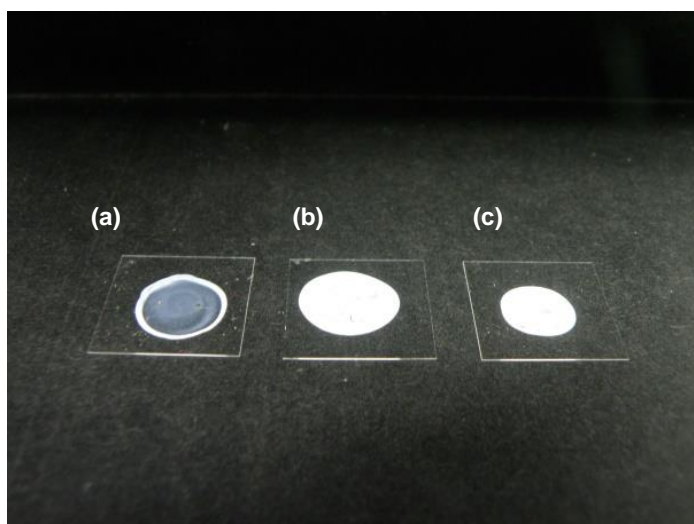


**Fig. S8** Photographs of (a)  $\alpha$ -, (b)  $\beta$ - and (c)  $\gamma$ -CD crystalline solids obtained after drying the HFIP solutions on a glass plate at ambient temperature.

## 7. XRD patterns of CD solids obtained by the freeze-drying of CD/HPIC solutions

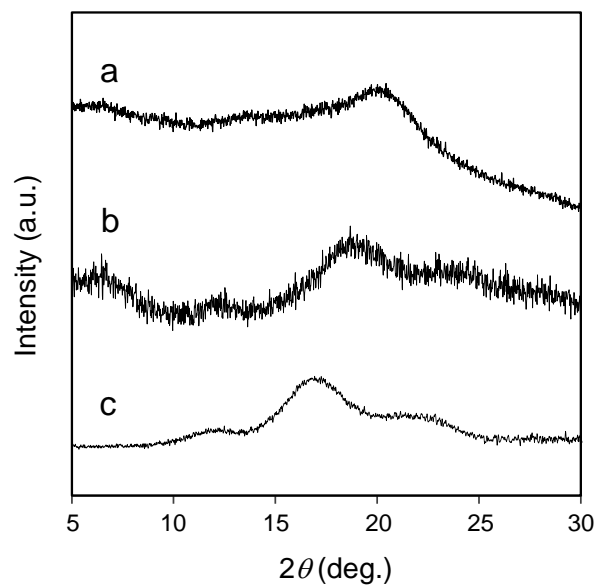


**Fig. S9** XRD patterns of (a)  $\alpha$ -, (b)  $\beta$ - and (c)  $\gamma$ -CD solids obtained by the freeze-drying of HFIP solutions (0.1 mol/L).

## 8. XRD patterns of the micrometer-sized CD beads formed by electrospinning of HFIP solutions

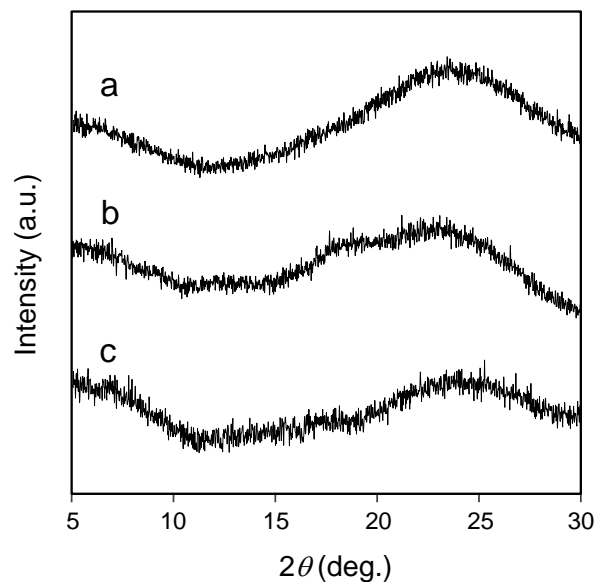


**Fig. S10** XRD patterns of (a)  $\alpha$ -, (b)  $\beta$ - and (c)  $\gamma$ -CD beads formed by electrospinning of HFIP solutions (2.5 wt%).

9. SEM image of  $\beta$ -CD structures formed by electrospinning of a 10 wt%  $\beta$ -CD/HFIP solution

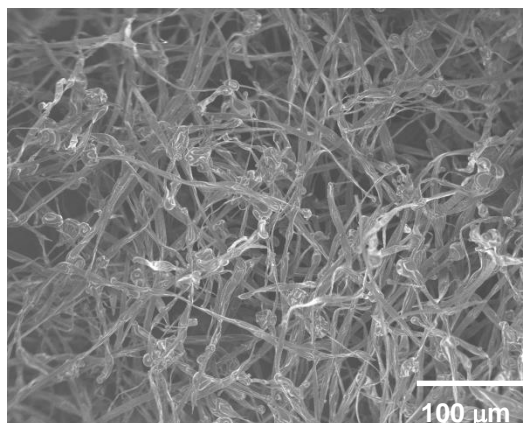


**Fig. S11** SEM image of  $\beta$ -CD structures formed by electrospinning of a  $\beta$ -CD/HFIP solution (10 wt%).